Chapter 5

Periodic Perturbations: Parametric Systems

Albert Morozov

Additional information is available at the end of the chapter

http://dx.doi.org/10.5772/intechopen.79513

Abstract

We are not going to present the classical results on linear parametric systems, since they are widely discussed in literature. Instead, we shall consider nonlinear parametric systems and discuss the conditions of new motion existence in the resonance zones: the regular ones (on an invariant torus) and the irregular ones (on a quasi-attractor). On the basis of the self-oscillatory shortened system which determines the topology of resonance zones, we study the transition from a resonance to a non-resonance case under a change of the detuning. We then apply our results to some concrete examples. It is interesting to study the behavior of a parametric system when the ring-like resonance zone is contracted into a point, i.e., to describe the bifurcations which occur in the course of transition from the plain nonlinear resonance to the parametric one. We are based on article, and we follow a material from the book.

Keywords: resonances, quasi-attractor, periodic solves, parametric perturbations

1. Introduction

Consider the following system:

$$\begin{aligned} \frac{dx}{dt} &= \frac{\partial H(x,y)}{\partial y} + \varepsilon g(x,y,\nu t), \\ \frac{dy}{dt} &= -\frac{\partial H(x,y)}{\partial x} + \varepsilon f(x,y,\nu t), \end{aligned} \tag{1}$$

where $\varepsilon > 0$ is a small parameter, ν is perturbation frequency, and g, f are continuous periodic functions of period 2π with respect to $\varphi = \nu t$. The Hamiltonian H as well as f and g will be assumed to be sufficiently smooth in a domain $G \subset R^2 \times S^1$ (or $G \subset R^1 \times S^1 \times S^1 = R^1 \times T^2$).

Also, we shall assume that the unperturbed ($\varepsilon = 0$) Hamiltonian system is nonlinear and has at least one cell D filled with closed phase curves.

We especially emphasize the following condition.

Condition A. $\frac{\partial g}{\partial x} + \frac{\partial f}{\partial y} \not\equiv 0$.

This implies that system (1) is nonconservative.

Along with (1), we shall consider the autonomous system:

$$\begin{aligned}\frac{dx}{dt} &= \frac{\partial H(x,y)}{\partial y} + \varepsilon g_0(x,y)\\ \frac{dy}{dt} &= -\frac{\partial H(x,y)}{\partial x} + \varepsilon f_0(x,y),\end{aligned} \tag{2}$$

where $g_0 = <g>_\varphi$ and $f_0 = <f>_\varphi$.

We also assume the following condition.

Condition B. System (2) has a finite set of rough limit cycles (LCs) in cell D.

Changing the variables x, y to the action I and angle θ, we obtain the system in the form

$$\begin{aligned}\dot{I} &= \varepsilon F_1(I,\theta,\varphi)\\ \dot{\theta} &= \omega(I) + \varepsilon F_2(I,\theta,\varphi)\\ \dot{\varphi} &= \nu,\end{aligned} \tag{3}$$

where

$$F_1 \equiv f x'_\theta - g y'_\theta, \quad F_2 \equiv -f x'_I + g y'_I \tag{4}$$

are periodic of period 2π with respect to θ and φ. System (3) is defined on the direct product $\Delta \times S^1 \times S^1 = \Delta \times T^2$, where T^2 is two-dimensional torus, $\Delta = \left(I^-, I^+\right), \quad I^\pm = I\left(h^\pm\right)$.

The definition of resonance. We say that in system (3) a resonance takes place if

$$\omega\left(I_{pq}\right) = (q/p)\nu, \tag{5}$$

where p, q are relatively prime integer numbers.

The energy level $I = I_{pq}$ ($H(x,y) = h_{pq}$) of the unperturbed system is called the resonance.

The behavior of solutions in the neighborhoods

$$U_\mu = \left\{(I,\theta) : I_{pq} - C\mu < I < I_{pq} + C\mu, \quad 0 \le \theta \le 2\pi, C = const\right\}, \quad \mu = \sqrt{\varepsilon}$$

of individual resonance levels $I = I_{pq}$ $\left(H(x,y) = h_{pq}\right)$ can be derived, up to the terms $O\left(\mu^2\right)$, from the pendulum-type equation [1, 2]

$$\frac{d^2v}{d\tau^2} - bA_0(v; I_{pq}) = \mu\sigma(v; I_{pq})\frac{dv}{d\tau}, \tag{6}$$

$$\begin{aligned} &b = d\omega(I_{pq})/dI, \tau = \mu t, A_0(v; I_{pq}) = \frac{1}{2\pi p}\int_0^{2\pi p} F(I_{pq}, v + q\varphi/p, \varphi)d\varphi, \\ &\sigma(v, I_{pq}) = \frac{1}{2\pi p}\int_0^{2\pi}\left(\frac{\partial g(x,y,\varphi)}{\partial x} + \frac{\partial f(x,y,\varphi)}{\partial y}\right)d\varphi, \end{aligned} \tag{7}$$

where $X = X(I_{pq}, v + q\varphi/p)$, $Y = Y(I_{pq}, v + q\varphi/p)$ is the unperturbed solution on the level $I = I_{pq}$. For nondegenerate resonance zones we consider here, it holds that $b \neq 0$. Functions $A_0(v; I_{pq})$, $\sigma(v; I_{pq})$ are periodic of period $2\pi/p$ with respect to v.

From Eq. (7) follows.

Theorem 1

If the divergence of the vector field of Eq. (6) depends on v, then the divergence of the vector field of the original system (1) contains terms which depend on both the time t and the spatial coordinates.

In many cases the converse is also true. For example, it holds for the system

$$dx/dt = y, \;\; dy/dt = -x - x^3 + (P_1 + P_2x^2 + P_3x\sin(\nu t))y + P_4\sin(\nu t). \tag{8}$$

The terms mentioned in Theorem 1 are called nonlinear parametric terms. Our goal is to study systems of the form (1) with such terms. The existence of those leads to new motions in resonance zones [1–3]. We shall demonstrate these motions on examples.

2. Investigation of Eq. (6)

The following representations hold:

$$\begin{aligned} &A_0(v; I_{pq}) = A_*(v; I_{pq}) + B(I_{pq}), \quad B =< A_0>_v, \\ &\sigma(v; I_{pq}) = \sigma_*(v; I_{pq}) + B_1(I_{pq}), \quad B_1 =< \sigma>_v, \end{aligned} \tag{9}$$

where $B(I)$ is the generating function of the autonomous system (2) and $B_1(I)$ is the derivative of $B(I)$. We shall focus on the case when σ is sign-alternating. In this case, from Eq. (9) follows the inequality:

$$|B_1(I_{pq})| < \max_v|\sigma_*(v, I_{pq})|. \tag{10}$$

When studying the pendulum Eq. (6), we shall distinguish two cases: (I) $B(I_{pq}) \neq 0$ and (II) $B(I_{pq}) = 0$.

In case II system (2) has a rough limit cycle (LC) in a neighborhood of the level $H(x, y) = h_{pq}$. There is no such cycle in case I.

Case I. Neglecting terms of order μ in Eq. (6), we arrive at the integrable equation

$$d^2v/d\tau^2 - bA_0(v, I_{pq}) = 0 \tag{11}$$

If $|B(I_{pq})| > max_v|A_*(v, I_{pq})|$, then Eq. (11) has no equilibrium states. The resonance level $I = I_{pq}$ is then referred to as passable. Note that the term "passable" has its origin in the topology of the resonance zone, as opposed to the same term used in physics, where "passing" stands for a change in perturbation frequency ν. In the case under consideration, there are no periodic solutions in the vicinity of the resonance level. The most interesting case is when Eq. (11) has equilibrium states, i.e., when the condition

$$|B(I_{pq})| < \max_v|A_*(v, I_{pq})| \tag{12}$$

is satisfied. The resonance level $I = I_{pq}$ is then said to be partly passable.

Under condition (10), Eq. (6) may have limit cycles. In order to find them, one must construct the Poincaré-Pontryagin generating function.

Figure 1(a) shows the phase portrait of Eq. (6) under conditions (10) and (12), and $p = 3$. On the period $2\pi/3$, there is a single limit cycle (note that on the period 2π (which is the period of the unperturbed solution) there are three limit cycles). If the cycle lies outside the neighborhood of the separatrix loop of Eq. (11), then there is a corresponding two-dimensional invariant torus in the original system. Since the period of the limit cycle of Eq. (11) is of order $O(1/\mu)$, we then have a long-periodic beating regime in the original system (6) (the generatrices of the torus are of different order).

However, if the limit cycle lies in the neighborhood of the separatrix loop, then the two-dimensional invariant torus in the original system (1) is destroyed. The bifurcation scene in which the cycle is caught into the separatrix loop is shown in **Figure 1(b)**. Taking into account the nonautonomous terms, which were discarded in deriving Eq. (6), leads to the homoclinic structure. Such a structure is shown in **Figure 1(c)** for the Poincaré map with $p = 3$. Because of

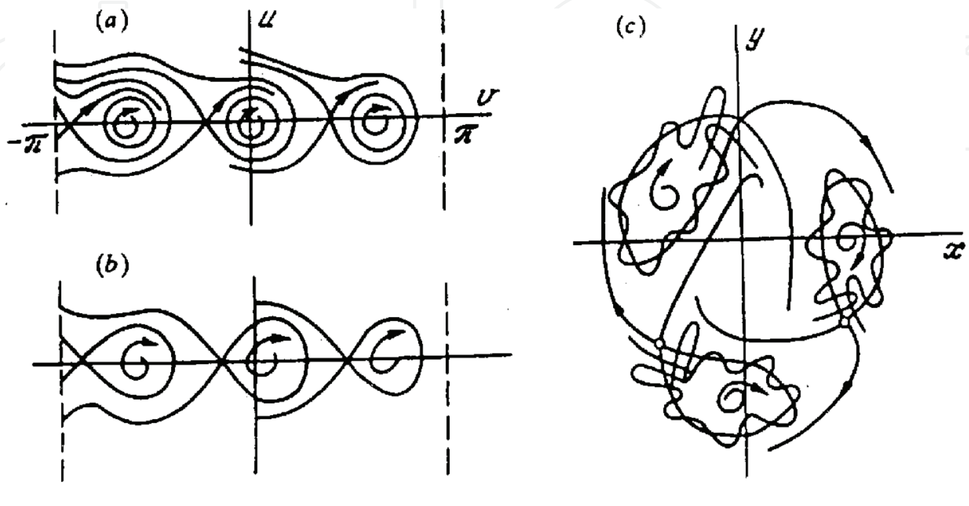

Figure 1. (a) Phase portrait of Eq. (6), (b) bifurcational case, and (c) Poincaré map for the initial system in case (b).

the presence of non-compact separatrices, in this case we merely have an irregular transition process.

Case II. Now, Eq. (6) always possesses equilibrium states, and we have the third kind of resonance zone, namely, an impassable zone. In order to better understand the structure of such a zone, we introduce in Eq. (6) the detuning γ between the level $I = I_{pq}$ and the level $I = I_0$, near which the autonomous system (2) has a limit cycle:

$$B(I_{pq}) = (dB(I_0)/dI)(I_{pq} - I_0) + O\left((I_{pq} - I_0)^2\right) \simeq \gamma\mu \tag{13}$$

Then, Eq. (6) can be rewritten as

$$\begin{aligned} du/d\tau &= A_*(v; I_{pq}) + \mu(\sigma(v; I_{pq})u + \gamma), \\ dv/d\tau &= bu. \end{aligned} \tag{14}$$

In Eq. (14) we change the variables from (u, v) to the action J and the angle L (in both the oscillatory and the rotational zones) and average the resulting system over the "fast" angular variable L. As a result, we arrive at the equation

$$\frac{dJ}{d\tau} = \mu b \mathbf{\Phi}(J)/2\pi,$$

where $\Phi(J)$ is the Poincaré-Pontryagin generating function [2] and it is discontinuous at $J = J_c$ when $\gamma \neq 0$. Here, J_c corresponds to the contour in the "unperturbed" system

$$\begin{aligned} du/d\tau &= A_*(v; I_{pq}), \\ dv/d\tau &= bu. \end{aligned} \tag{15}$$

formed by the saddle and two separatrix loops embracing the phase cylinder.

We shall therefore use Melnikov's formula [4] to determine the relative position of the separatrices which in the shortened system (15) constitute the contour formed by the outer separatrix loops:

$$\begin{aligned} &\Delta = \mu\Delta_1^{\mp} + O(\mu^2) \\ &\Delta_1^{\mp} = b\textstyle\int_{-\infty}^{\infty}\left(\sigma_*(v_0; I_{pq}) + B_1(I_{pq})\right)u_0^2 d\tau \mp 2\pi\gamma. \end{aligned}$$

Here, v_0, u_0 is the solution of Eq. (15) on the contour consisting of the saddle and the outer separatrix loops. Setting $d = \max_v|\sigma_*(v; I_{pq})| = \|\sigma_*\|$, $a = |B_1(I_{pq})|/d$ we find from the formula for $\Delta_1^{\pm}$ that $\Delta_1^{\pm} = d(\alpha + \beta a) \pm 2\pi\gamma$, where

$$\alpha = b\int_0^{\infty} \overline{\sigma}(v_0; Ipq)u_0^2 d\tau, \beta = b\int_0^{\infty} u_0^2 d\tau, \overline{\sigma} = \frac{\sigma_*}{\|\sigma_*\|}.$$

From the condition $\Delta_1^{\pm} = 0$, we get

$$\gamma = \gamma^{\pm} = \mp d(\alpha + \beta a)/2\pi. \tag{16}$$

In system (14) the upper contour exists when $\gamma = \gamma^{+}$, and the lower contour when $\gamma = \gamma^{-}$. Eq. (16) defines two straight lines in the (a, γ) plane. They intersect each other at $(a^{*}, 0)$, where $a^{*} = -\alpha/\beta$. When $|a| > 1$ the function $\sigma(v; I_{pq})$ is sign-preserving, and when $|a| < 1$ it is sign-alternating.

In virtue of Eq. (10), the second case is the most interesting. The case $|a| < 1$ is somewhat special since system (14) may then have limit cycles in both the oscillatory and rotational domains, which have no generating counterparts in system (2). Limit cycles in Eq. (14) can result from the following phenomena [5]: (a) from a degenerate focus, (b) from a separatrix loop (contour), and (c) from a condensation of trajectories. However, if the number of limit cycles does not matter, it suffices to consider the case when there is no more than one limit cycle in the oscillatory domain. Then, we can make a general conclusion on the change of qualitative dynamics of Eq. (14) under variation of the detuning. However, beforehand, we should study the problem for the case when f and g are trigonometric polynomials of degree N in φ. Then, A_{*} and σ_{*} are also trigonometric polynomials of degree $N_1 \leq N$:

$$\begin{aligned} -bA_{*}(v; I_{pq}) &= \sum_{i=1}^{N_1} (a_i \cos(ipv) + b_i \sin(ipv)) \\ \sigma_{*}(v; I_{pq}) &= \sum_{i=1}^{N_1} (d_i \cos(ipv) + c_i \sin(ipv)). \end{aligned} \tag{17}$$

From the definition of functions $A_{*}(v)$ and $\sigma(v)$ (see Eq. (7)), it follows that, in general, different harmonics in the perturbation contribute to A_{*} and σ. This means that different harmonics can dominate in Eq. (17). We count only these main harmonics in Eq. (17) (for $A_{*} \Rightarrow 1$ and $\sigma_{*} \Rightarrow n$). We then derive from Eq. (6) the equation

$$z'' + \sin(z) = \mu\left[(\cos(nz) + a)z' + \gamma\right], \tag{18}$$

where $z = pv + \psi, \quad \psi = \arctan(b_1/a_1)$.

The generating function $\Phi(J)$ for Eq. (18) can be presented as [3]

$$\begin{aligned} &\Phi(J(\rho)) = \Phi^{(s)}(\rho) = aF_n^{(s)}(\rho) + F_0^{(s)}(\rho) \pm \delta_{2s} 2\pi\gamma \\ &F_0^{(1)}(\rho) = 16[(\rho - 1)\mathbf{K} + \mathbf{E}], F_1^{(1)}(\rho) = 16[(1 - \rho)\mathbf{K} + (2\rho - 1)\mathbf{E}]/3, \\ &F_0^{(2)}(\rho) = 8\mathbf{E}/\sqrt{\rho}, F_1^{(2)}(\rho) = 8[2(\rho - 1)\mathbf{K} + (2 - \rho)\mathbf{E}]/3\rho^{3/2} \end{aligned} \tag{19}$$

where $s = 1$ corresponds to the oscillatory domain and $s = 2$ to the rotational domain. $\mathbf{K}$, $\mathbf{E}$ are the complete elliptic integrals with modulus k ($\rho = k^2$). Note that $\rho = (1 + \tilde{h})/2$ in the oscillatory domain and $\rho = 2/(1 + \tilde{h})$ in the rotational domain, and $\tilde{h} = \tilde{h}(J(\rho))$ is the value of the energy integral of the equation $z'' + \sin(z) = 0$. Function $F_j^{(s)}(\rho)$ is the generating function defined by the perturbation term $z^{'}\cos(jz)$. The plus in Eq. (19) corresponds to the upper half of the cylinder, the minus to the lower half, and δ is the Kronecker delta. This enables us to find all the bifurcation sets (except the one corresponding to a contractable separatrix loop) explicitly [6].

We shall first consider the case when $\gamma = 0$. In this case Eq. (18) is identical to the standard equation [2], and $\Phi(\rho)$ is continuous at $\rho = 1$. Thus, it determines the limit cycles up to the separatrix. This case was considered in **Figure 2(a–e)** that the rough topological structures are shown for $n = 1$. Note that the limit cycles can "disappear at infinity" only when $B_1 = 0$. This is impossible when Condition B is satisfied. **Figure 2(e)** shows the bifurcation when the limit cycle "clings" to the separatrix contour ($\Phi(\rho)$ has the simple root $\rho = 1$). **Figure 2(f)** shows the corresponding behavior of the invariant curves (separatrices) of the Poincaré map for the original system with $p = 3$. The neighborhood of the homoclinic contour is attracting. Moreover, a complicated structure exists in the neighborhood [7], and, consequently, we have a quasi-attractor, i.e., a nontrivial hyperbolic set, and stable points can exist in it.

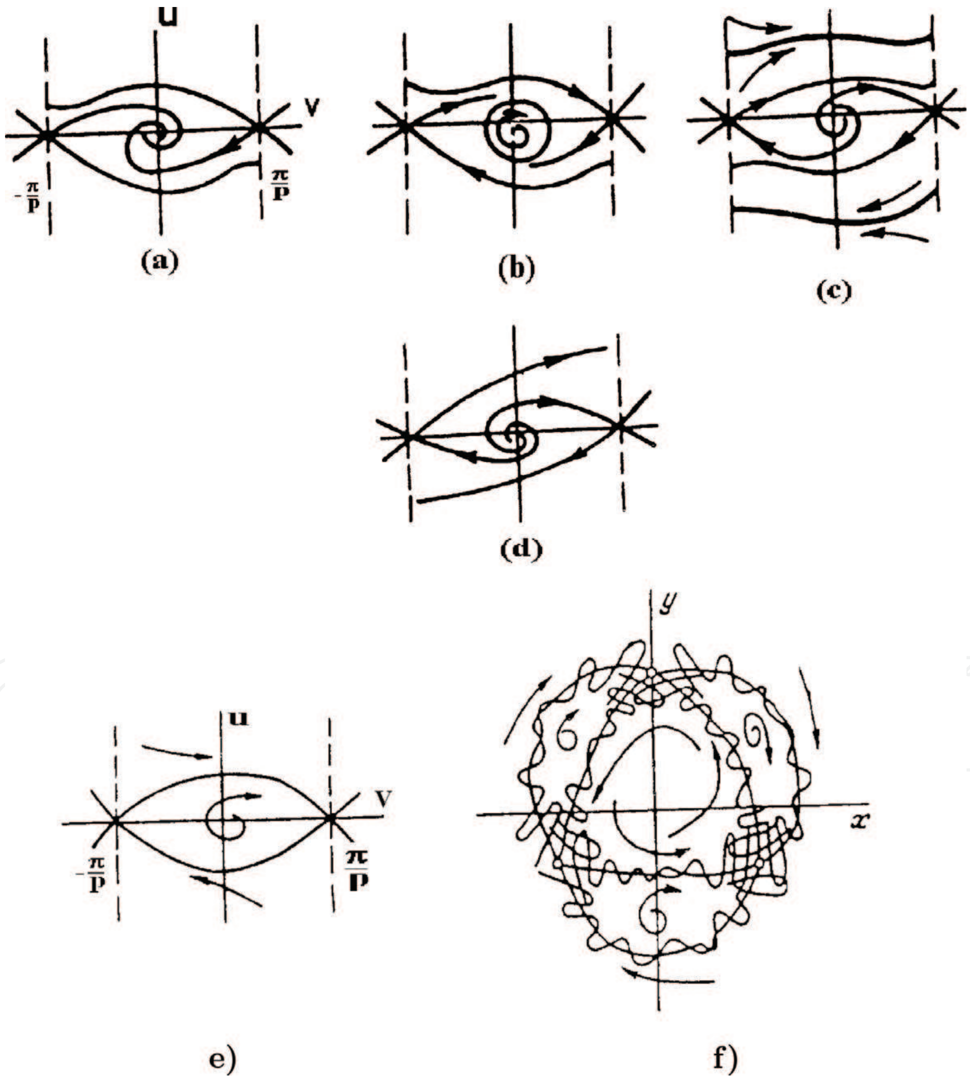

Figure 2. Phase portraits of Eq. (18) (a–e) and the Poincare map (f) for the case (e) and $p = 3$.

When $\gamma \neq 0$ the generating function $\Phi(\rho)$ is discontinuous at $\rho = 1$. The bifurcation of the cycle clinging to the separatrix must, therefore, be considered separately.

Using Melnikov's formula, we compute $\Delta_1^{\pm}$, which measures the split of the unperturbed separatrix for Eq. (18). One can see that equation $\Delta_1^{\pm} = 0$ is equivalent to $\Phi^{(2)}(1) = 0$. Then, using Eq. (19) and assuming (for concreteness) $n = 1$, we find the bifurcational values $\gamma^{\pm} = \mp 4(a + 1/3)/\pi$. When $\gamma = \gamma^{+} + O(\mu)$, we have a non-contractable separatrix loop lying in the domain $z' \geq 0$, and when $\gamma = \gamma^{-} + O(\mu)$, we have a loop in the domain $z' \leq 0$. From Eq. (19) we obtain the asymptotic formula, $\Phi^{(2)}(\rho) \simeq \pi\left(8a/\sqrt{\rho} + \sqrt{\rho} \pm 4\gamma\right)/2$, as $\rho \to 0$. This implies that the straight line $a = 0$ in the plane (a, γ) is singular. Furthermore, from Eq. (19) we find in the parametric form the line of the double cycles:

$$a = a_0(\rho) = -\left(F^{(2)}\right)'/\left(F^{(2)}\right)', \quad \gamma = \gamma_0(\rho) = \mp\left(F^{(2)}\left(F_n^{(2)}\right)' - \left(F^{(2)}\right)'F^{(2)}\right)/2\pi \cdot \left(F^{(2)}\right)',$$
$$\rho \in [0, 1], \quad \text{or} \quad \gamma = \gamma_0^{\pm}(a).$$

It is observed that the transformation of the phase portrait of Eq. (18) for $\rho \cong 1$ involves the creation of a contractable separatrix loop. By Condition B, we have $a \neq 0$, which implies that the saddle number is nonzero. The separatrix loop can, therefore, give rise to one limit cycle only [5]. The corresponding bifurcational set $\gamma_1^{\pm}(a)$ in the parameter plane can be found numerically.

We thus obtain a partition of the parameter plane (a, γ) into domains corresponding to different topological structures for Eq. (18), as well as the structures themselves (they are shown in **Figure 3**) for $n = 1$. The structures corresponding to cases 8–12 are not shown in **Figure 3**, since they can be obtained from structures 5, 6, 3, 2, and 14, respectively, by the directions of the coordinate axes.

Note that, along with a non-contractable separatrix loop, Eq. (18) has either a stable limit cycle, or a stable equilibrium state, or the stable "point at infinity." This means that no quasi-attractor can exist in the original nonautonomous system when $\gamma \neq 0$. Remark that the homoclinic structure exists for a small range of γ values $\left(|\gamma - \gamma^{\pm}| \simeq \exp(-1/\mu)\right)$.

Those limit cycles of Eq. (18) which do not lie in the neighborhood of the unperturbed separatrix contour correspond to the two-dimensional invariant tori in the original system (like in the case $B \neq 0$). Unlike when $B \neq 0$, two kinds of such tori may exist in Eq. (18) corresponding to the limit cycles in the oscillatory and rotational domains. The tori corresponding to the cycles in the rotational domain (with one exception) have no generating "Kolmogorov torus" in the perturbed Hamiltonian system, while the (asymptotically stable) tori corresponding to the limit cycles in the oscillatory domain are images of the tori occupying the next level in the hierarchy of resonances.

Remark The cases of odd and even n should be considered separately. When n is even, an unstable cycle clings to the separatrix loop. For odd n the same thing happens to a stable cycle. Only the case of odd n is therefore interesting when one studies the problem of existence of a quasi-attractor.

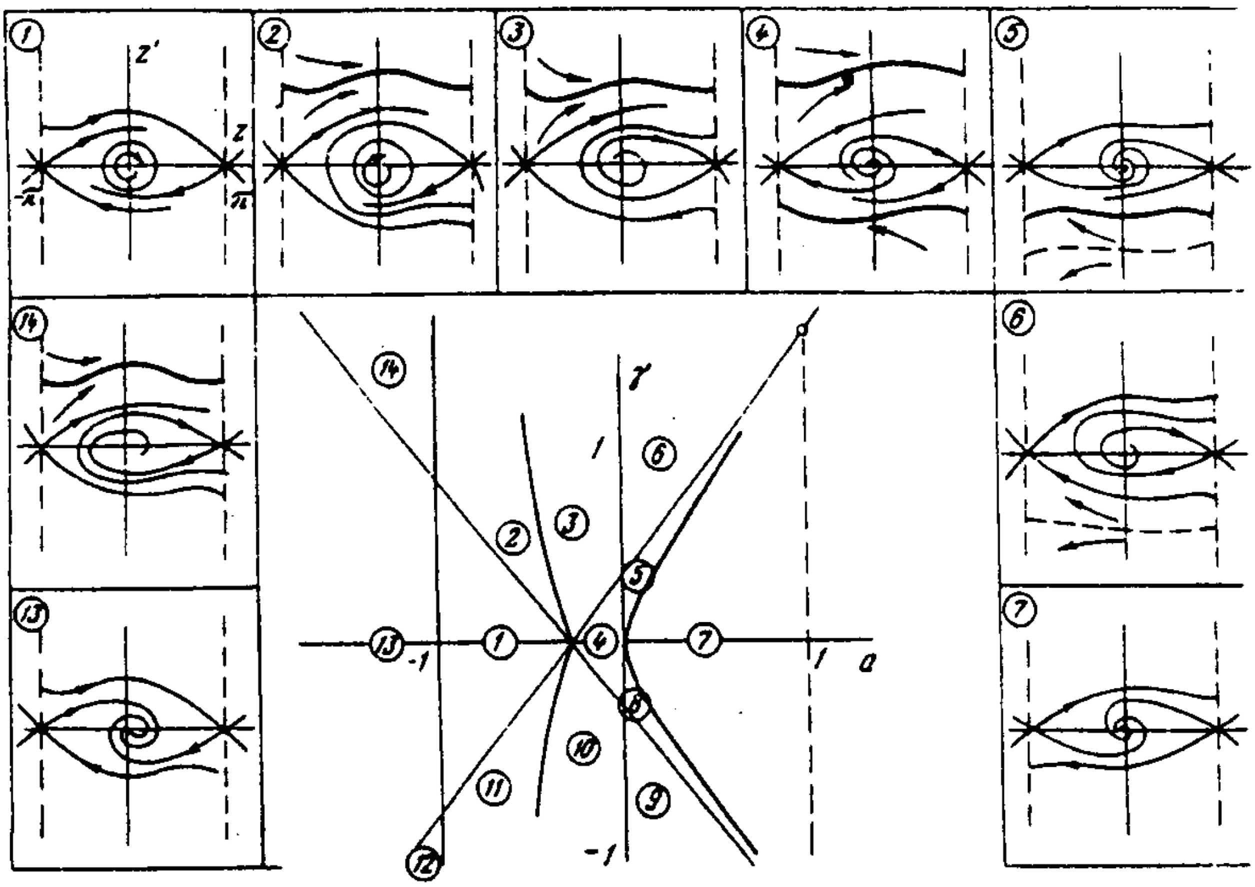

Figure 3. Bifurcation diagram and the corresponding rough phase portraits of Eq. (18).

According to the bifurcation diagram (**Figure 3**), it is convenient to break the case $|a| < 1$ into three sub-cases: (a) $-1 < a < a_*$, (b) $a_* < a < 0$, and (c) $0 < a < 1$, $a_* = 1/\left(1 - 4n^2\right)$. Let n be odd. Then considering the solutions on the original cylinder $\{v(\mathrm{mod}2\pi), u\}$, we derive the following theorem.

Theorem 2

There are μ_*, $\gamma^{\pm}(a)$, $\gamma_0^{\pm}(a)$, $\gamma_1^{\pm}(a)$, and a_* such that, if $|\mu| < \mu_*$ and n are odd, the following three intervals of a (in Eq. (18)) can be chosen: 1°. $a \in (-1, a_*)$; 2°. $a \in (a_*, 0)$; and 3°. $a \in (0, 1)$.

1. *Let $a \in (-1, a_*)$. Then, (1) when $\gamma > \gamma_1^+ > 0$, Eq. (14) has exactly one stable limit cycle (LC) in the rotational domain and no more than $p(n-1)$ LCs in the oscillatory domain (OD); (2) when $\gamma_1^+ < \gamma < \gamma^+$, there are p additional LCs in the OD, which are born from the separatrix loops at $\gamma = \gamma_1^+$; (3) when $\gamma = \gamma^+$, the stable LC in the rotational domain clings to the separatrix contour Γ_p^+ consisting of p saddles and their outer separatrices going from one saddle to another, while the "free" unstable separatrices approach an LC in the OD; (4) when $\gamma^- < \gamma < \gamma^+$, there are no LCs in the rotational domain and no more than pn LCs in the OD; (5) when $\gamma = \gamma^-$, there appears a separatrix contour Γ_p^- which consists of p saddles and their outer separatrices but has orientation and location different from those of Γ_p^+; (6) when $\gamma_1^- < \gamma < \gamma^-$, there are no more than pn LCs in*

the OD and one stable non-contractible LC; and (7) when $\gamma < \gamma_1^-$, Eq. (14) has one stable non-contractible LC which lies in the lower half-cylinder $u < 0$ and no more than $p(n-1)$ in the OD.

2. *Let $a \in (a_*, 0)$. Then, in the OD there are $p(n-1)$ LCs, and in the rotational domain, (1) when $\gamma > \gamma^-$, Eq. (14) has one stable LC for $u > 0$; (2) when $\gamma = \gamma^-$, a contour Γ_p^- appears; (3) when $\gamma^+ < \gamma < \gamma^-$, one stable LC exists on the upper half-cylinder $(u > 0)$ and one stable LC on the lower half-cylinder $(u < 0)$; (4) when $\gamma = \gamma^+$, a contour Γ_p^+ appears; and (5) when $\gamma < \gamma^+$, one stable LC exists for $u < 0$.*

3. *Let $a \in (0, 1)$. Then, there are at most $p(n-1)$ LCs in the OD, and in the rotational domain, (1) when $\gamma > \gamma^-$ and $u < 0$, Eq. (14) has one stable LC; (2) when $\gamma = \gamma^-$, a contour Γ_p^- appears; (3) when $\gamma_0^- < \gamma < \gamma^-$ and $u < 0$, there is a stable LC born from Γ_p^- and an unstable LC; (4) when $\gamma = \gamma_0^-$, the stable and unstable LCs merge together; (5) when $\gamma_0^+ < \gamma < \gamma_0^-$, no LCs exist; (6) when $\gamma = \gamma_0^+$, a semi-stable LC is formed for $u > 0$; (7) when $\gamma^+ < \gamma < \gamma_0^+$, one stable and one unstable LCs exist for $u > 0$; (8) when $\gamma = \gamma^+$, a contour Γ_p^+ is formed; and (9) when $\gamma < \gamma^+$, one unstable LC exists for $u > 0$.*

3. Example 1

Consider system (8) which is equivalent to the equation [3]

$$\ddot{x} + x + x^3 = \left(P_1 + P_2 x^2 + P_3 x \sin(\nu t)\right)\dot{x} + P_4 \sin(\nu t), \tag{20}$$

where P_i, $(i = 1, 2, 3, 4)$ are parameters. Here, we focus only on the effects which are due to the nonlinear parametric term $x\dot{x}\sin(\nu t)$. Let us assume $\nu = 4$. Then, for small $P_i (i = 1, 2, 3, 4)$ system (20) can have only two "splittable" resonance levels: $H(x, y) = h_{11}, H(x, y) = h_{31}$ and $h_{31} < h_{11}$. The corresponding autonomous system $(P_3 = P_4 = 0)$ has at most one LC. The passage of this LC through the resonances under a change of parameter P_2 was considered in [2]. If this LC lies outside the neighborhoods of resonance levels $H(x, y) = h_{11}, H(x, y) = h_{31}$, then in the original nonautonomous system (20), there is a two-dimensional invariant torus T^2 corresponding to the cycle. There is a generating "Kolmogorov torus" in the Hamiltonian system $(P_1 = P_2 = P_3 = 0)$.

A computer program was developed by the author for a simulation of Eq. (20). The results of such simulation are presented in **Figures 4–6**. In the numerical integration, the Runge-Kutta-type formulae are used with an error of order $O(h^6)$ per integration step h. In **Figure 4(a)** we present the Poincaré map for $P_1 = 0.0472$, $P_2 = -0.008$, and $P_3 = 0.018$, which determines the structure of the main resonance zone $(p = 1, q = 1)$. Along with the separatrices of the saddle fixed point S, a closed invariant curve encircling the unstable fixed point O is shown, which corresponds to a stable LC in the oscillatory domain of Eq. (6). This closed invariant curve appears for $P_3 \approx 0.014$ when the fixed point O loses its stability. As P_3 increases, so does the size of the closed invariant curve, and for $P_3 \approx 0.0487$ the curve clings to the separatrix of

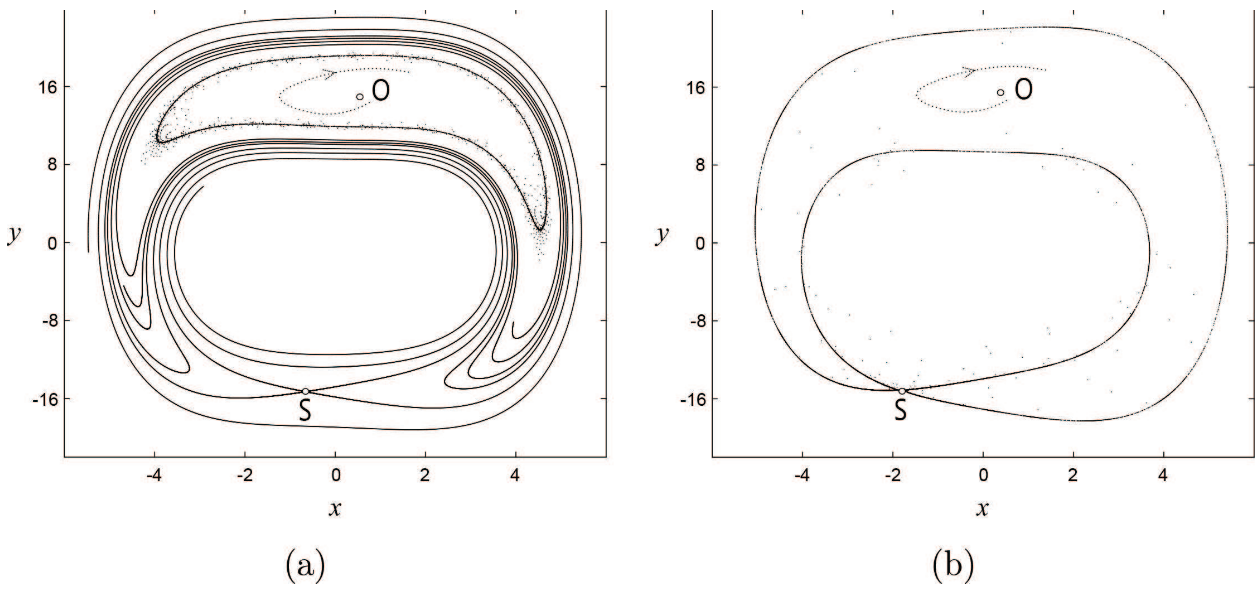

Figure 4. Poincaré map for Eq. (20) with $P_1 = 0.0472$, $P_2 = -0.008$, $P_4 = 2$, and $\nu = 4$ and (a) $P_3 = 0.018$ and (b) $P_3 = 0.0489755$.

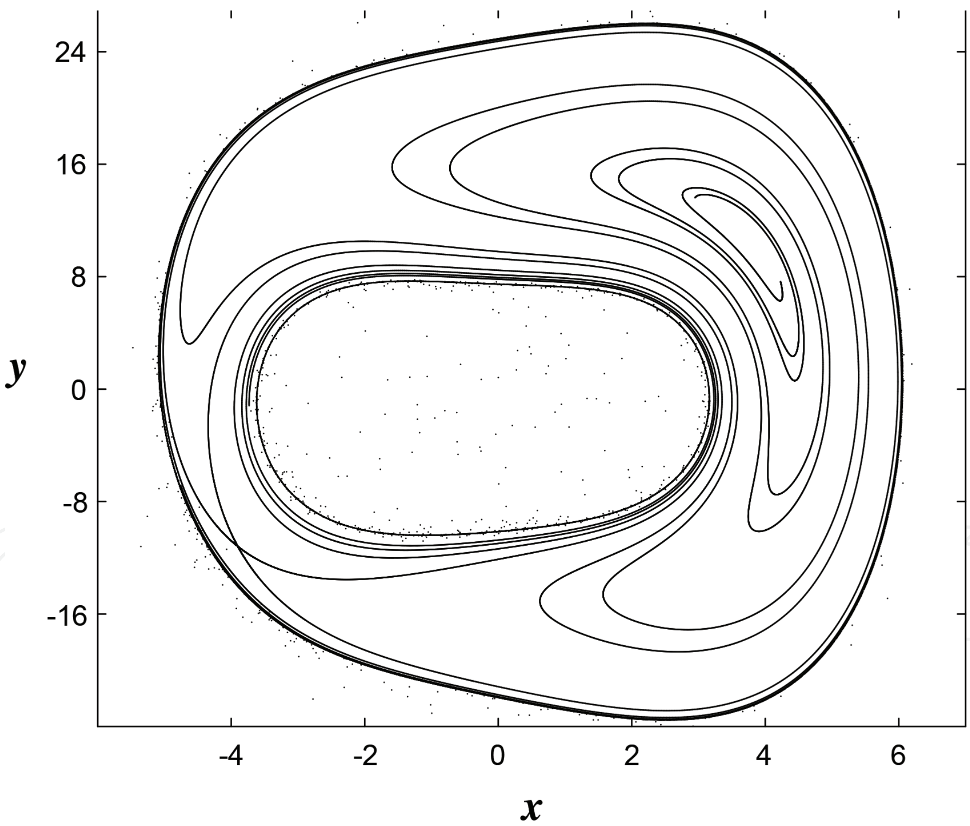

Figure 5. Poincaré map for Eq. (20) with $P_1 = 0.0472$, $P_2 = -0.008$, $P_3 = 0.15$, $P_4 = 2$, and $\nu = 4$.

the saddle point S, forming a contour (see **Figure 4(b)**). As P_3 increases further, two closed invariant curves appear, shown in **Figure 5** for $P_3 = 0.15$. The structural changes of the resonance zone observed in the experiment are in good agreement with the theoretical results for $\gamma = 0$. The observations for $\gamma \neq 0$ are consistent with the theory, too.

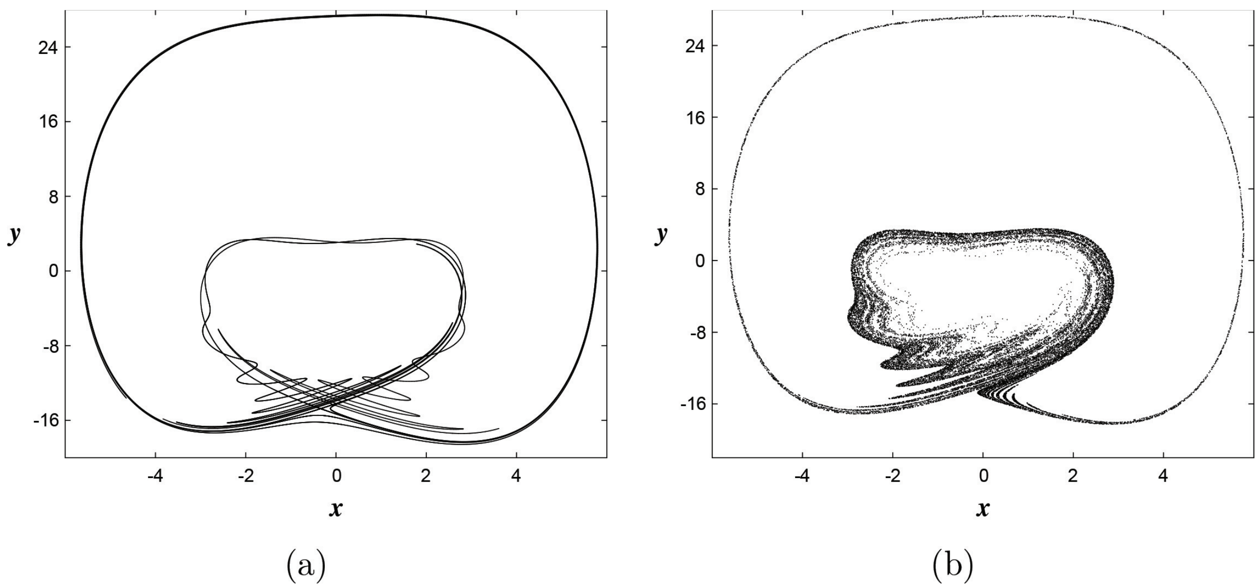

Figure 6. Poincaré map for Eq. (20) with $P_1 = 0.0472$, $P_2 = -0.008$, $P_3 = 0.0487$, $P_4 = 8$, and $\nu = 4$ (a) and quasi-attractor (b).

In the case presented in **Figure 6**, the transversal intersection of the separatrices of S cannot be detected visually. We, therefore, increased P_4 to obtain a better picture of the homoclinic structure. When $P_4 = 8$, the structure can be seen clearly (**Figure 6(a)**). The corresponding quasi-attractor is the only attracting set (**Figure 6(b)**). Stable periodic points with long periods can exist inside the quasi-attractor itself. However, they are extremely difficult to detect numerically.

4. Example 2

As opposed to Example 1, this one pursues a different goal, namely, to study the transition from the classical parametric resonance to the nonlinear resonance. One of the problems for which this can be done is that of the pendulum with a vibrating suspension.

The pendulum with vibrating suspension is a classical example of a problem in which a parametric resonance can be observed. A large number of publications (see, e.g., [8, 9]) are devoted to this problem. Other problems of this sort include the bending oscillations of straight rod under a periodic longitudinal force [10], the motion of a charged particle (electron) in the field of two running waves [11], etc. The parametric resonance in this kind of systems appears when a fixed point of the corresponding Poincaré map loses its stability and is, therefore, usually described by the linearization near this point.

It is interesting to study the behavior of a parametric system when the ring-like resonance zone is contracted into a point, i.e., to describe the bifurcations which occur in the course of transition from the plain nonlinear resonance to the parametric one. This paragraph is devoted to the solution of this problem in the case of a nonconservative pendulum with a vertically oscillating suspension.

http://dx.doi.org/10.5772/intechopen.79513

The motion of the pendulum with vertically oscillating suspension (under some simplifying assumptions) is described by the equation [13]

$$\ddot{x} + \sin x + p_1 \cos\beta t \sin x + p_2 \dot{x} = 0, \tag{21}$$

where p_1, p_2, β are parameters.

Let us now complicate the model even more and consider the equation

$$\ddot{x} + \sin x + p_1 \cos\beta t \sin x + (p_2 + p_3 \cos x)\dot{x} = 0, \tag{22}$$

with the phase space $\mathbf{R}^1 \times \mathbf{S}^1 \times \mathbf{S}^1$. The term $p_3 \dot{x} \cos x$ appears, for example, in the case of the pendulum in which the force of resistance is created by a vertical plate perpendicular to the plane of oscillations. Consider Eq. (22) when it is close to integrable, i.e., for small values of parameters $p_i (i = 1, 2, 3)$. Denote $p_i = \varepsilon C_i$, where ε is a small parameter. Then, the original Eq. (22) takes the form

$$\ddot{x} + \sin x = \varepsilon\left[C_1 \cos\beta t \sin x + (C_2 + C_3 \cos x)\dot{x}\right], \tag{23}$$

Eq. (23) in the conservative case, when $C_2 = C_3 = 0$, is considered in many publications. For instance, for small angles of the deviation x, the case $\beta \cong 2$ is studied in [8]. The criterion of resonance overlap is applied in [11] to estimating the width of the "ergodic layer." The existence of homoclinic solutions is discussed in [12] without the assumption on smallness of parameter ε.

Phase curves of the unperturbed mathematical pendulum equation are determined by the integral $H(x, \dot{x}) \equiv \dot{x}^2 - \cos x = h$, where $h \in (-1, 1)$ in the oscillatory domain and $h > 1$ in the rotational domain. The peculiarity lies in the way period τ depends on h in the oscillatory domain.

We have

$$\begin{aligned} &\tau(h) = 2\pi/\omega = 4\mathbf{K}(k), k^2 = (1 + h)/2, \ -1 < h < 1, \\ &\tau(h) = 2k\mathbf{K}, k^2 = 1/(1 + h), h > 1. \end{aligned} \tag{24}$$

Here, $\mathbf{K} = \mathbf{K}(k)$ is the complete elliptic integral of the first kind, k being its modulus. From Eq. (24) it follows that the period τ changes noticeably only for h close to 1, i.e., in the neighborhood of the separatrix. Therefore, small intervals of period τ, which determines the width of resonance zones, correspond to fairly large intervals of variable x.

4.1. Structure of resonant zones

In the investigation of the perturbed equation, we first focus on the structure of resonance zones in domains $G^1 = \{(x, \dot{x}) : -1 < h_- \le H(x, y) \le h_+ < 1\}$ and $G^2 = \{(x, \dot{x}) : H(x, y) \ge h_* > 1\}$. The resonance condition $\tau(h_{pq}) = (p/q)(2\pi/\beta)$, where p, q are relatively prime integers, determines the resonance levels of energy $H(x, y) = h_{pq}$.

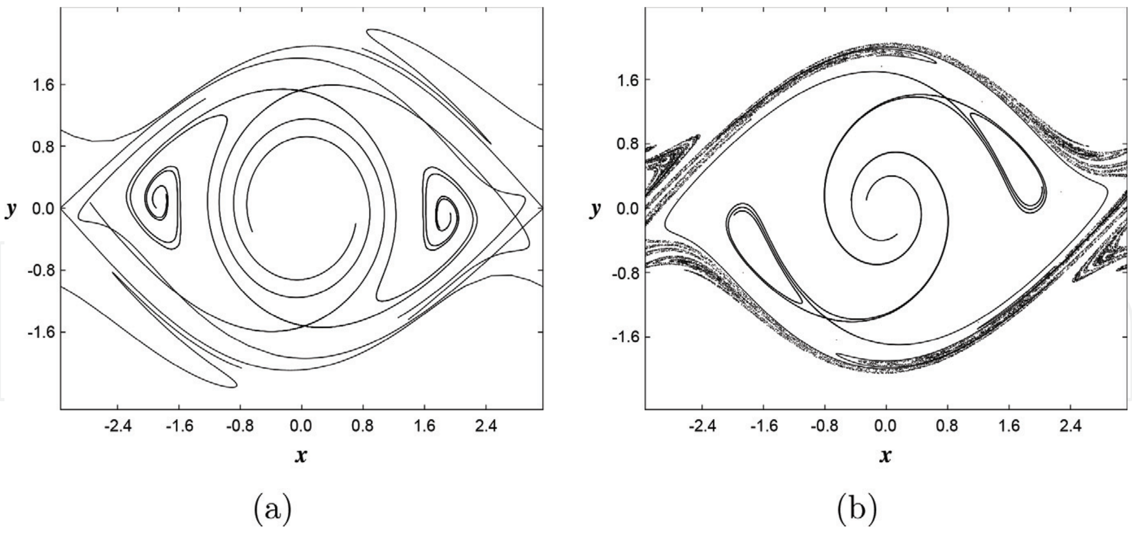

Figure 7. Invariant curves (separatrices) of Poincaré map for Eq. (22) with $p_1 = -0,1$, $p_3 = 0,1$, $\beta = 1.6$, and $p_2 = -0,07$ (a) with $p_2 \simeq -1/30$ (b).

The structure of individual resonance zones U_μ is described (up to the terms $O(\varepsilon^{3/2})$) by the pendulum-type Eq. (6). Since functions A_0 and σ have different forms in the oscillatory and rotational domains, we introduce the notations $A_0^{(s)}(v, h_{pq})$ and $\sigma^{(s)}(v, h_{pq})$, where $s = 1$ corresponds to the oscillatory domain and $s = 2$ to the rotational one.

In our case the divergence of the vector field of Eq. (23) contains no terms explicitly depending on t; hence, σ does not depend on v, i.e., $\sigma = \text{const}$.

The functions $A_0^{(s)}$ and $\sigma^{(s)}$ in an explicit form were obtained in [13]. It is also found that the width of the resonance zone decreases rapidly with the increase of p when $q = 1$.

A computer-generated picture of invariant curves of the Poincaré map for Eq. (22), with $\beta = 1.6$, is shown in **Figure 7**. In Eq. 21(a) a case of synchronization of oscillations in the subharmonic with $p = 2, q = 1$ ($p_1 = 0,1$, $p_2 = 0,07$, $p_3 = -0,1$) is shown, and in **Figure 7(b)**, a partly passable resonance with $p = 2, q = 1$ $(p_1 = 0,1, p_2 = 1/30, p_3 = -0,1)$ is shown. In the domain G^2 the synchronization of oscillations on the main resonance ($p = q = 1$) takes place.

4.2. Neighborhood of the origin

Denote $U_n = \{(x,y) : 0 \le H(x,y) \le C\varepsilon^{2/n}\}$ and substitute in Eq. (23):

$$x = \varepsilon^{1/n}\xi, \;\; y = \dot{x} = \varepsilon^{1/n}\eta$$

As a result, we arrive at the system

$$\begin{aligned} &\dot{\xi} = \eta, \;\; \dot{\eta} = -\xi + \varepsilon\left[C_1\xi\cos(\beta t) + (C_2 + C_3)\eta\right] + \varepsilon^{2/n}\xi^3/6- \\ &-\varepsilon^{1+2/n}\left(C_1\xi^3\cos(\beta t)/6 + \xi^2\eta\right) + \dots \end{aligned} \tag{25}$$

System (25) is defined in $D \times \mathbf{S}^1$ where D is a certain domain in $\mathbf{R}^2$. In the neighborhood $U_1\,(n = 1)$, system (25) assumes the form

$$\dot{\xi} = \eta, \;\; \dot{\eta} = -\xi + \varepsilon\left[C_1 \cdot \xi \cdot \cos(\beta t) + (C_2 + C_3)\eta\right] + O\left(\varepsilon^2\right). \tag{26}$$

By discarding in Eq. (26) the terms $O\left(\varepsilon^2\right)$, we arrive at the Mathieu equation with the extra term resulting from the viscous friction. It is clear that in the framework of a linear equation one cannot observe the (nonlinear) effects which accompany the transition from the nonlinear resonance to the parametric one. So, let us consider a wider neighborhood $U_2\,(n = 2)$ of the origin. In Eq. (25) we discard the terms $O\left(\varepsilon^2\right)$ and, for the resulting system, consider the resonance cases when $\omega = 1 = q\beta/p$ (p and q being relatively prime integers). We then study the bifurcations pertaining to the transition from the parametric resonance to the ordinary one. We once again introduce the detuning $1 - q\beta/p = \gamma_1\varepsilon$. As a result, the system in question will be rewritten as

$$\begin{aligned} \dot{\xi} &= (q\beta/p)\eta + \gamma_1\varepsilon \\ \dot{\eta} &= -(q\beta/p)\xi + \varepsilon\left[C_1\xi\cos\beta t + (C_2 + C_3)\eta - \gamma_1\xi + \xi^3/6\right]. \end{aligned} \tag{27}$$

Now, we introduce the action (I) – angle (ϑ) variables. Since the unperturbed system is linear, the substitution has the simple form $\xi = \sqrt{2I}\sin\vartheta$ and $\eta = \sqrt{2I}\cos\vartheta$. In terms of this variables, system (27) will be written as

$$\dot{I} = \varepsilon F(I, \vartheta, \varphi), \;\; \dot{\vartheta} = q\beta/p - \varepsilon R(I, \vartheta, \varphi), \;\; \dot{\varphi} = \beta, \tag{28}$$

where $F = 2IG\cos\vartheta - \gamma_1\sqrt{2I}\sin\vartheta$, $R = G\sin\vartheta + \gamma_1\cos\vartheta/\sqrt{2I}$

$$G = C_1\sin\vartheta\cos\varphi + (C_2 + C_3)\cos\vartheta - \gamma_1\sin\vartheta + (I/3)\sin^3\vartheta.$$

Let us introduce in Eq. (28) the "resonance phase" $\psi = \vartheta - q\varphi/p$ and average the resulting system over the "fast" variable φ. As a result, we arrive at the two-dimensional autonomous system

$$\begin{aligned} \dot{u} &= \varepsilon[C_1/2)u\sin 2v + (C_2 + C_3)u] \\ \dot{v} &= \varepsilon\left[(C_1/4)\cos 2v - u/8 - \gamma_1/2\right] \end{aligned} \tag{29}$$

when $p = 2$ and $q = 1$ and to the system

$$\begin{aligned} \dot{u} &= \varepsilon(C_2 + C_3) \\ \dot{v} &= \varepsilon\left(-u/8 - \gamma_1/2\right) \end{aligned} \tag{30}$$

when $p \neq 2$ and/or $q > 1$. As we know, $u = I + O(\varepsilon), \quad v = \psi + O\left(\varepsilon^2\right)$. From Eq. (29) and (30), it follows that (in our approximation) only one resonance with $p = 2, q = 1$ appears in the neighborhood U_2.

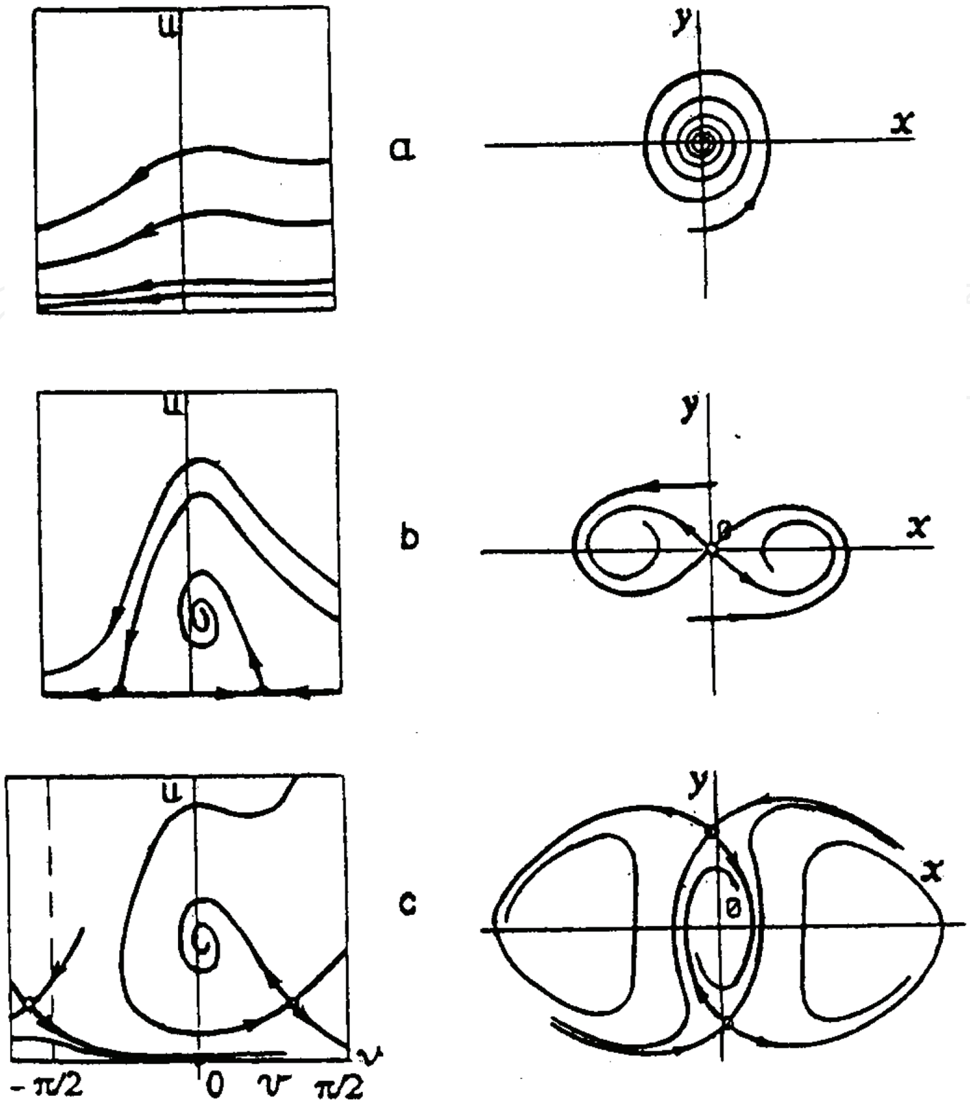

Figure 8. Phase portraits of system (29) with $C_2^2 + C_3^2 \neq 0$.

The investigation of system (29) when $C_2^2 + C_3^2 \neq 0$ for different values of detuning γ_1 presents no difficulty, because, according to the Bendixson criterion, there are no limit cycles. The most typical rough phase portraits are presented in **Figure 8** where, parallel with the phase portraits in the (u, v) plane, the corresponding phase portraits in Cartesian coordinates $(x, y = \dot{x})$ are shown. **Figure 8(a)** corresponds to the case when we have $\gamma_1 > \gamma_* > 0$, $\gamma_* = \sqrt{C_1^2 - 4(C_2 + C_3)^2}/2$, **Figure 8(b)** when $|\gamma_1| \leq \gamma_*$, and **Figure 8(c)** when $|\gamma_1| > \gamma_*$ and $\gamma_1 < 0$. In addition, in all three cases, we assume $C_2 + C_3 < 0$.

4.3. Conclusion

The number of splittable resonances is bounded, when $C_2^2 + C_3^2 \neq 0$. For the actual pendulum (Eq. (22)), when the small nonconservative forces are present, we, most likely, have one resonance regime with $p = 2, q = 1$ in the oscillatory domain and the one with $p = 1, q = 1$ in the rotational domain.

In conclusion we make the following remarks on Eqs. (22) and (23).

1. The transition from **Figure 8(a)–(c)** corresponds to two period-doubling bifurcations, while the passage from the parametric resonance (**Figure 8(b)**) to the ordinary nonlinear resonance (**Figure 8(c)**) corresponds to the birth of two periodic (of period 2) saddle points and a node (focus) from a multiple saddle fixed point.
2. The bifurcation which involves the birth of a quasi-attractor (**Figure 7(b)**) in the neighborhood of the unperturbed separatrix is the most interesting one. It may take place at any magnitude of the external force (parameter C_1). It suffices to have $B^{(s)}(1) = 0, (C_2 = -C_3/3), \varepsilon(C_2 - C_3) < 0$, for example, $C_2 = -1/30, C_3 = 0.1, \varepsilon > 0$..
3. In the quasi-integrable nonconservative case, there appear no resonances with $q > 1$ and odd p in the oscillatory domain and no resonances with $q > 1$ and even p in the rotational domain.

Acknowledgements

This work was supported in part by the Russian Foundation for Basic Research under grant no. 18-01-00306, by the Russian Science Foundation under grant no. 14-41-00044.

Author details

Albert Morozov

Address all correspondence to: morozov@mm.unn.ru

Lobachevsky State University of Nizhny Novgorod, Russia

References

[1] Morozov AD, Shil’nikov LP. On nonconservative periodic systems similar to two-dimensional Hamiltonian ones. Pricl. Mat. i Mekh. (Russian). 1983;**47**(3):385-394

[2] Morozov AD. Quasi-conservative systems: Cycles, resonances and chaos. World Scientific Series on Nonlinear Science Series A. 1998;**30**. http://www.worldscientific.com/worldscibooks/10.1142/3238

[3] Morozov AD. Resonances and chaos in parametric systems. Journal of Applied Mathematics and Mechanics. 1994;**58**(3):413-423

[4] Melnikov VK. On stability of a center under periodic in time perturbations. Work of the Moscow Mathematical Society. 1963;**12**:3-52

[5] Andronov AA, Leontovich EA, Gordon II, Maiyer AG. The Theory of Bifurcations of Dynamical Systems in a Plane. Moscow, Russia: Publ. Nauka; 1967

[6] Morozov AD, Dragunov TN. Visualization and the Analysis of Dynamic Systems. Moscow-Izhevsk: Publ. Institute of Computer Researches; 2003

[7] Shil'nikov LP. About the Poincaré-Birkgof problem. Mathematical Reviews. 1997;**174**(3): 378-397 Russian

[8] Struble RA. Oscillations of a pendulum under parametric excitation. Quarterly of Applied Mathematics. 1963;**21**(2):121-131

[9] Struble RA, Marlin JA. Periodic motion of a simple pendulum with periodic disturbance. Quarterly Journal of Mechanics and Applied Mathematics. 1965;**18**(4):405-417

[10] Bolotin VV. Dynamic Stability of Elastic Systems. Moscow: Gostehizdat; 1956 (Russian)

[11] Zaslavsky GM, Chirikov BV. Stochastic unstability of nonlinear oscillations. Uspekhi Fizicheskikh Nauk (Russian). 1971;**105**(1):3-39

[12] Cherry TM. The asymptotical solutions of the analytical hamiltonian systems. Journal of Differential Equations. 1969;**4**(2):142-156

[13] Morozov AD. The problem of pendulum with an oscillating point of suspension. Journal of Applied Mathematics and Mechanics. 1995;**59**(4):563-570